Biosensors and Bioelectronics 77 (2016) 157–163

Contents lists available at ScienceDirect

Biosensors and Bioelectronics

journal homepage: www.elsevier.com/locate/bios

Lable-free quadruple signal amplification strategy for sensitive electrochemical p53 gene biosensing

Zonghua Wang *,1, Jianfei Xia *,1, Daimin Song, Feifei Zhang, Min Yang, Rijun Gui, Lin Xia, Sai Bi, Yanzhi Xia

Laboratory of Fiber Materials and Modern Textile, The Growing Base for State Key Laboratory, College of Chemical Science and Engineering, Shandong Sino-Japanese Center for Collaborative Research of Carbon Nanomaterials, Collaborative Innovation Center for Marine Biomass Fiber Materials and Textiles, Qingdao University, Qingdao, Shandong 266071, China

ARTICLE INFO

Article history:
Received 10 June 2015
Received in revised form
22 August 2015
Accepted 4 September 2015
Available online 14 September 2015

Keywords:
Signal amplification
Label-free
Electrochemical
DNA biosensor
Target recycling
G-quadruplex-hemin DNAzyme

ABSTRACT

A versatile label-free quadruple signal amplification biosensing platform for p53 gene (target DNA) detection was proposed. The chitosan–graphene (CS–GR) modified electrode with excellent electron transfer ability could provide a large specific surface for high levels of AuNPs-DNA attachment. The large amount of AuNPs could immobilize more capture probes and enhance the electrochemical signal with the excellent electrocatalytic activity. Furthermore, with the assist of N.BstNB I (the nicking endonuclease), target DNA could be reused and more G-quadruplex-hemin DNAzyme could be formed, allowing significant signal amplification in the presence of H_2O_2. Such strategy can enhance the oxidation–reduction reaction of adsorbed methylene blue (MB) and efficiently improve the sensitivity of the proposed biosensor. The morphologies of materials and the stepwise biosensor were characterized by scanning electron microscopy (SEM), transmission electron microscopy (TEM) and cyclic voltammetry (CV). Differential pulse voltammetry (DPV) signals of MB provided quantitative measures of the concentrations of target DNA, with a linear calibration range of 1.0×10^{-15}–1.0×10^{-9} M and a detection limit of 3.0×10^{-16} M. Moreover, the resulting biosensor also exhibited good specificity, acceptable reproducibility and stability, indicating that the present strategy was promising for broad potential application in clinic assay.

1. Introduction

The p53 gene, a tumor suppressor, plays critical roles in many cellular anti-cancer mechanisms and is known as “the guardian of genome” (Lee et al., 2009; Chen et al., 2010). If this gene is mutated, it can speed up tumor growth. The development of a feasible, reliable and sensitive strategy for the detection of p53 gene, especially at ultra-low physiological concentrations, has been of great significance. Owing to its inherent advantages such as simplicity, sensitivity, rapidness and low cost, to date, considerable attentions have been given to the electrochemical technique in DNA detection (Paleček and Bartošík, 2012). Furthermore, in order to realize the ultrasensitive detection, many efforts have been made for developing novel electrochemical biosensors based on various target amplification and signal amplification principles.

As for the target amplification, the polymerase chain reaction (PCR) method for DNA monitoring exhibits limitations such as complexity, potential contamination and high cost (Lee et al., 1993). The rolling circle amplification (RCA) shows some improvement, but still encounters problems such as hash reaction conditions and costly polymerase (Li et al., 2010). On this occasion, nuclease assisting target recycling was put forward. So far, various smart nuclease including restriction endonucleases (Chen et al., 2013; Zhu et al., 2014) and exonucleases (Wang et al., 2014; Liu et al., 2013a, 2013b) have been applied for bioanalytical applications. Among them, the nicking endonuclease signal amplification (NESA) as a newly developed technique attracted researchers' attention to design sensitive biosensors of target DNA for their autonomous circular amplification and simple operations (Miao et al., 2013; Zhang et al., 2014b). As one of the nicking endonuclease, N.BstNB I enzyme cleaves only one strand of a double stranded DNA four bases away from the 3'-end of its recognition sequence (5′-GAGTC-3′), which have been used extensively (Zhou et al., 2013).

On the other hand, signal amplification principles often realized by nanomaterials. One major merit is that one can control and tailor their properties in a predictable manner to meet the

* Corresponding authors. Fax: +86 532 85950873.
E-mail addresses: wangzonghua@qdu.edu.cn, 13853219173@126.com (Z. Wang).
[1] These authors contributed equally to the present study.

http://dx.doi.org/10.1016/j.bios.2015.09.011
0956-5663/

needs of specific applications. Furthermore, the integration of nanomaterials with functional DNA has provided new hybrid systems (Rosi and Mirkin, 2005). Among various nanomaterials, gold nanoparticles (AuNPs), with huge reactive surface area, unusual catalytic property and biocompatibility, were often used to prepare aptamer-conjugated AuNPs for detection of biomolecules (Wu et al., 2013; Deng et al., 2013; Jungemann et al., 2013). And the formed DNA-AuNP conjugates have been utilized as amplifying labels for novel biosensing protocols owning to their unique physical and chemical features, such as multivalent binding capability, enhanced affinity, excellent catalytic properties for signal amplification (Qiu et al., 2013; Xu et al., 2013).

In order to further push down the detection limit, another nanomaterial, graphene (GR), with the structure of a single-atom-thick sheet of sp^2-bonded carbon atoms in a closely packed honeycomb two-dimensional lattice, has draw a lot of attention. Considering its biocompatibility (Chen et al., 2008), GR is an ideal material utilized for improved performance of biosensors attributed to synergistic effect of GR and accompanying material in the nanocomposite (Yao et al., 2012). Furthermore, the high surface area of GR is helpful in increasing the surface loading of the molecules. Because of the low electronic noise from thermal effect, GR-based chemical sensors can also have a much higher sensitivity (He et al., 2012). Moreover, the excellent conductivity and small band gap are favorable for conducting electrons from the biomolecules (Brownson et al., 2012). However, GR tends to form agglomerates. Thus, the successful dispersion of GR has enabled the construction of various potentially useful GR-based biosensors. Chitosan (CS), a semi-synthetically derived aminopolysaccharide with many admirable properties (Erdem et al., 2014; Singh et al., 2013), is commonly used to disperse nanomaterials for constructing biosensors (Kang et al., 2009). As it is a polycationic polymer (Erdem et al., 2014), it can adhere to negatively charged GR to form a well dispersed and stable CS–GR nanocomposite. Furthermore, the existence of CS on GR can provide a good biocompatible microenvironment (Kang et al., 2009).

More recently, considerable research efforts have been directed toward the application of DNAzymes, a new effective biocatalyst in biorecognition and biosensing events as an electrocatalytic label (Pelossof et al., 2010, 2012; Zhou et al., 2012). As one of the most classic DNAzyme, G-quadruplex-hemin complex, which is composed of a single-stranded guanine-rich nucleic acid and hemin, has horseradish peroxidase-like activity and shows great catalytic activity to H_2O_2 (Deng et al., 2008). Several advantages over natural peroxidases, such as their small size, high chemical and thermal stability, low cost and easy synthesis (Breaker, 2000) makes G-quadruplex-hemin complex a very attractive biocatalysts for amplified biosensing applications and a novel kind of catalytic label for the development of DNA biosensors (Liu et al., 2014; Gao and Li, 2013). Moreover, many researchers have combined methylene blue (Zhang et al., 2014a), alcohol (Zheng et al., 2014), thionine (Yuan et al., 2015) with G-quadruplex-hemin to construct novel biosensing platform, in which the changes of current are triggered by the catalysis of G-quadruplex-hemin to H_2O_2 and NADH.

To significantly improve the detection sensitivity for p53 gene, herein, a highly sensitive and selective sensing strategy based on the combination of quadruple signal amplifications, AuNPs, GR, the N.BstNB I-assisted target recycling and G-quadruplex-hemin DNAzyme catalyzing was proposed. By the assisting of the excellent signal generation catalyzed by the G-quadruplex-hemin DNAzyme, our method is exempt from conventional cumbersome labeling and is essentially simple and convenient by exploiting the inherent advantages of electrochemistry as well. The proposed label-free and quadruple signal amplification approach for DNA detection showed a high sensitivity, wide detection range and excellent specificity, and thus possesses promise for sensing application.

2. Experimental section

2.1. Materials and reagents

Methylene blue (MB) was purchased from Aladdin. Tris-(2-carboxyethyl) phosphine (TCEP), tris(hydroxymethyl) aminomethane (Tris) and hemin were obtained from Sangon Biotech Co., Ltd. Chitosan (CS), acetic acid and glutaraldehyde (GLU) were purchased from Tianjin reagent chemicals Co., Ltd. Graphite powder was provided by Qingdao Fujin graphite Co., Ltd. Graphene (GR) was synthesized by the modified Hummers method (Wang et al., 2012). Gold(III) chloride trihydrate ($HAuCl_4 \cdot 3H_2O$) was purchased from Sinopharm Chemical Reagent Beijing Co., Ltd. AuNPs (about 13 nm) were prepared by means of citrate reduction of $HAuCl_4$ according to the literature (Liu and Lu, 2006). The nicking endonuclease (N.BstNB I) and 10 × NEBuffer 3 (50 mM Tris–HCl, 10 mM $MgCl_2$, 100 mM NaCl, pH 7.9) were obtained from New England BioLabs (Ipswich, MA, USA). All the other chemicals were of analytical grade and used as received. The synthesized oligonucleotides were obtained from Sangon Biotech Co., Ltd. (Shanghai, China). All the oligonucleotides solutions were heat-treated in 90 °C for 3 min and then cooled in ice for 10 min prior to use. The sequences are listed as follows:

S1: 5′-NH_2-C6-TTT TTT T*CT GAC GCT GCT CAC G*-3′

S2: 5′-SH-C6-TTT TT*C GTG AGC AGC GTC AG*-3′ (The italic letters are complementary with the italic letters of S1)

Hairpin capture probe (CP): 5′-SH-C6-AAA GGG TTG GGC GG*G ATG GGT T*<u>**GA GTC**</u> **TTC C↓AG TGT GAT GA***A ACC CAT C*-3′ (The italic letters are the sequence of the stem arms; the underlined letters are the recognition sequence of N.BstNB I, and the arrow indicates the nicking position; the bold letters are complementary with the target DNA)

5′-NH_2-C6-AAA GGG TTG GGC GG*G ATG GGT T*<u>**GA GTC**</u> **TTC C↓AG TGT GAT GA***A ACC CAT C*-3′ for comparison biosensor fabrication

p53 gene target (TD): 5′-TCA TCA CAC TGG AAG ACT C-3′

Single-base mismatch target (sTD): 5′-TCA TCA CAC TGG AAG A<u>A</u>T C-3′

Non-complementary target (nTD):5′-GAC GTC AGA CTT CCT GCG A-3′.

2.2. Apparatus

CV and DPV were performed at room temperature (RT) on a CHI-660C electrochemical workstation (Chenhua Instrument Co., Ltd., Shanghai, China) coupled with a conventional three-electrode configuration where modified glassy carbon electrode (GCE, 3 mm in diameter) was used as working electrodes, platinum wire as an auxiliary electrode and saturated calomel as a reference electrode (SCE). The morphologies of materials were characterized by SEM (JSM-6700F) and TEM (JEM-2100). Absorption spectra were measured on a UV-2800A ultraviolet–visible (UV–vis) spectrophotometer (Unico Instrument Co., Ltd., Shanghai, China)

2.3. Synthesis of S2 and CP functionalized AuNPs

Initially, a mixture of 0.6 nM S2 and 2.4 nM CP was directly injected into 1000 μL gold colloids in a NaOH-treated glass vial (before conjugation, S2 and CP should be pretreated by TCEP to split the formed disulfide between the thiolated DNA probes). After gently shaking, the mixture was transferred to the refrigerator at 4 °C for further reaction (overnight). Then, added 10 μL 500 mM Tris–HCl (pH 7.4) and 115 μL 1 M NaCl dropwise

with gentle shaking. Stored the vial at 4 °C for least another day before use. Following that, the mixture was centrifuged (13,000 g) for 15 min. The nanoparticles (designed as S2-CP-AuNP) was re-suspended in 200 μL 100 mM Tris–HCl (pH 7.4, 100 mM NaCl), and centrifuged again. Finally, the nanoparticles were dispersed in 500 μL 100 mM Tris–HCl (pH 7.4, 300 mM NaCl), and stored at 4 °C until use.

2.4. Fabrication of biosensor

The GCE was polished with 0.05 μm and then 0.3 μm alumina slurries and rinsed thoroughly with double distilled water. After sonicated in ethanol and deionized water successively, the electrode was rinsed with double distilled water, and finally dried under an infrared lamp. GR (3 mg) was dispersed in 1.5 mL of 0.2 wt% CS solution (dissolved in 1% acetic acid) with ultra-sonication to form the CS–GR suspension for further characterization and application. The CS–GR/GCE was prepared by casting 6 μL of as-prepared suspension onto the surface of GCE and dried in air.

S1 was covalently immobilized on CS–GR/GCE using GLU. CS–GR/GCE was placed in 2.5% GLU for 2 h and then washed with 0.1 M NaOH and washing buffer (10 mM Tris–HCl, pH 7.4). Activated electrode was then soaked in 0.5 μM S1 for 1 h. The fabricated S1/CS–GR/GCE was then thoroughly washed with washing buffer and stored at 4 °C until use.

S2-CP-AuNP was assembled to the surface of modified electrode via immersing the S1/CS–GR/GCE into 30 μL S2-CP-AuNP for the formation of ds-DNA structures between S1 and S2. The hybridization reaction was carried out for 1 h at 40 °C. Subsequently, the electrode was thoroughly rinsed with washing buffer. The obtained electrode was named as S2-CP-AuNP/S1/CS–GR/GCE.

As comparisons, biosensors fabricated without GR or AuNPs, which named as S2-CP-AuNP/S1/GCE and CP/CS–GR/GCE, were fabricated as follows: (1) S2-CP-AuNP/S1/GCE. The GCE was oxidized at +1.5 V for 30 s in an aqueous solution containing 85 mM K_2CrO_7 and 1.7 M HNO_3 to produce more carboxyl group. After rinsed, the electrode was activated in 20 mM Tris–HCl (pH 7.4) containing 20 mM EDC and 10 mM NHS at 4 °C for 2 h (Xu et al., 2006) to activate carboxyl groups. The electrode was rinsed again and soaked in S1 solution to form the S1/GCE. S2-CP-AuNP was immobilized on the S1/GCE by hybridization between S1 and S2 as the S2-CP-AuNP/S1/CS–GR/GCE fabrication. (2) CP/CS–GR/GCE. CS–GR/GCE was activated with GLU and then treated with NH_2-CP to form the CP/CS–GR/GCE.

To monitor the each step for immobilization, the measurements of CV was performed in 0.1 M of KCl aqueous solution containing 5 mM of $[Fe(CN)_6]^{3-/4-}$ as the probe and recorded with a step potential of 1 mV in the potential range of −0.3 to 0.6 V at a scan rate of 100 mV/s. And the experimental parameters mentioned above, including of solution concentrations, temperatures and times, were optimized.

2.5. DNA hybridization and the nicking reaction

The prepared biosensor was reacted with 50 μL of TD with different concentrations. Upon incubation at 40 °C for 80 min, the sensor was incubated in a solution of N.BstNB I reaction buffer (0.5 U/μL) in 50 μL NEBuffer 3 at 55 °C for 60 min. Then the solution was heated to 90 °C and kept for 10 min to deactivate the N. BstNB I enzyme. After cooling down to room temperature, the biosensor was rinsed with washing buffer and incubated in hemin solution of 0.2 mM to form G-quadruplex-hemin DNAzyme at room temperature (RT) for 30 min. The biosensor was further dipped in 0.5 mM MB aqueous solution for 50 min at RT. The signal was monitored by DPV in 100 mM Tris–HCl (pH 7.4) containing 0.1 M KCl and 2 mM H_2O_2 from −0.5 to 0 V with the parameters of increment potential, 0.004 V; pulse amplitude, 0.05 V; pulse width, 0.05 s; sample width, 0.0167 s; pulse period, 0.2 s; quiet time, 2 s. After each step, the biosensor was washed with washing buffer. Analyses are always made in triplicate.

3. Results and discussion

3.1. Sensing mechanism

The principle of the sensing mechanism in this work is illustrated in Fig.1. Via electrostatic interaction, GR was noncovalently functionalized with CS. The fabricated CS–GR/GCE provided a large specific surface for high levels of DNA S1 loading, with the assist of GLU. Hemin-based hairpin CP and S2 functionalized AuNPs was prepared through the classical Au-S bond. With the hybridization between S1 and S2, the S2-CP-AuNP/S1/CS–GR/GCE was fabricated. Owning to the high specific surface area of AuNPs, many hemin-binding hairpin CP can be introduced into the biosensor. As the N.BstNB I is specifically designed to recognize specific nucleotide sequences in double-stranded DNA (ds-DNA) and cleaves only one of the two strands. In the absence of TD, the N.BstNB I cannot nick the hairpin CP and a part of the G-rich nucleic acid sequence yields a stable duplex domain in the stem region of the hairpin which eliminates the formation of the active G-quadruplex-hemin structure when the hemin and K^+ are added in the test system. However, when a perfectly matched TD hybridizes to the hairpin DNA, the stem of the hairpin CP is opened and a full recognition site will form for N.BstNB I. Then the N.BstNB I binds to and nicks the cleavage site. After nicking, the hairpin CP is cleaved into two fragments, and only the G-rich sequence remains on the electrode surface. Subsequently, the released target DNAs again hybridize with other hairpin CP and initiate the target recycling cycles, resulting in the cleavage of many hairpin CP and the formation of many G-quadruplex-hemin DNAzyme with the help of the hemin and K^+. In this way, a single target can activate many G-quadruplex-hemin DNAzymes. Meanwhile, MB, as an electrochemical indicator, is abundantly adsorbed on the oligonucleotides via specific interaction of MB with guanine base and served as an electron mediator. During the electrochemical measurement, each MB (as a good electron mediator) can produce an electrochemical signal with the applied potentials. Meanwhile, the formed G-quadruplex-hemin DNAzyme can further catalyze the reduction of H_2O_2 with the aim of dramatically improving the oxidation–

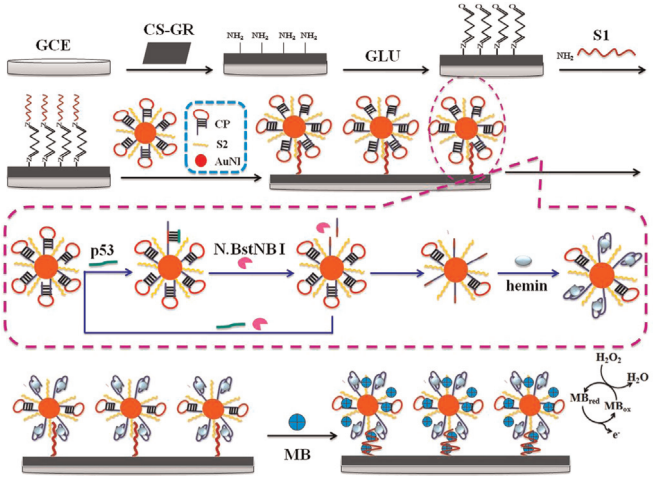

Fig.1. Schematic routine of the biosensor fabrication and its signal amplification strategy for p53 gene detection based on CS–GR, AuNPs, nicking endonuclease and G-quadruplex-hemin DNAzyme.

reduction reaction of MB (Yuan et al., 2013; Xu et al., 2013), thus leading to an amplified electronic signal. By monitoring the change in the current, we can indirectly determine the concentration of TD in the sample.

3.2. Material characterizations

Fig. S1A shows the SEM image of CS–GR composite, clearly clarifying the typical crumpled and wrinkled flake-like sheet structure. The TEM images of AuNPs and S2 and CP functionalized AuNPs are shown in Fig. S1B and C, respectively. The border of the AuNPs was clear while that of the S2-CP-AuNPs was ambiguous, which was caused by the functionalization of nucleotides on the surface of AuNPs. The UV–vis absorption spectra showed that the maximum absorption of the AuNPs was observed at 520 nm and it was red-shifted to 524 nm for S2-CP-AuNPs, which further confirmed that the AuNPs were successfully assembled with S2 and CP (Fig. S1D).

3.3. Electrochemical characterization of the stepwise modified electrodes

Fig. S2 describes CVs of bare GCE (a), CS–GR/GCE (b), S1/CS–GR/GCE (c), S2-CP-AuNP/S1/CS–GR/GCE (d) in 0.1 M KCl and 5 mM of $[Fe(CN)_6]^{3-/4-}$. It is observed that, redox peak currents increases for CS–GR/GCE as compared to bare GCE. The increase in peak current for CS–GR/GCE is attributed to uniformly distributed GR in CS that provides high surface area, excellent electrical conductivity and electron mobility at RT. On the other hand, peak broadening in terms of peak separation potential (ΔE_p) from 0.098 V for GCE to 0.213 V of CS–GR indicates that the electron transfer process is not reversible. Peak current decreases on subsequent functionalization of the electrode with S1 with the help of GLU is attributed to masking of electroactive surface by GLU which is insulating in nature and leads to perturb the electron communication. After immobilization of S2-CP-AuNP onto GLU functionalized CS–GR/GCE peak current rises and can be ascribed to increased charge transfer owing to ionic conductance and π–π interaction of DNA (Johnson et al., 2008). Besides this, sugar phosphate backbone of DNA being negatively charged is usually surrounded by positive "counter ions". This may form DNA/water/counter ion complex that will attract more negatively charged $[Fe(CN)_6]^{3-/4-}$ which in turn will contribute to increase in redox current.

3.4. Signal amplification component

Fig. 2 shows the DPVs of different modified electrodes in a 100 mM Tris–HCl solution containing 0.1 M KCl and 2 mM H_2O_2. A small current was obtained for S2-CP-AuNP/S1/CS–GR/GCE (curve a). In the presence of hemin and N.BstNB I but without TD (curve b), or in the presence of N.BstNB I and TD but without hemin (curve c), or in the presence of hemin and TD but without N.BstNB I (curve d), there were no significant changes in the peak currents compared with curve a, suggesting that G-quadruplex-hemin DNAzyme was not formed. In the absence of TD, hairpin CP, which contained a large number of G based in the stem region, could not become duplex for N.BstNB I nicking which eliminates the formation of the active G-quadruplex-hemin structure when the hemin and K^+ are added in the test system. Additionally, G-quadruplex-hemin DNAzyme cannot form without hemin or N.BstNB I. In the absence of G-quadruplex-hemin DNAzyme, H_2O_2 could not play a role, as a result of which, the electrochemical responses did not obviously change when using MB as an electron mediator (Zhang et al., 2013). With hemin, N.BstNB I and TD (curve e), the peak DPV current increased significantly, indicating that a large amount of G-quadruplex-hemin DNAzyme formed with the help of the nicking endonuclease N.BstNB I. Therefore, N.BstNB I was adopted in this system for signal amplification.

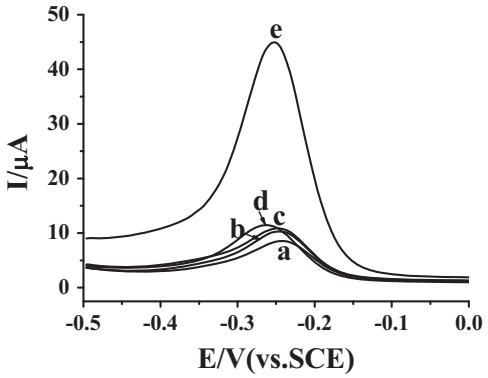

Fig. 2. DPVs of S2-CP-AuNP/S1/CS–GR/GCE (a); the electrode (a) in the presence of hemin and N.BstNB I, but without TD (b); the electrode (a) in the presence of N. BstNB I and TD, but without hemin (c); the electrode (a) in the presence of hemin and TD, but without N.BstNB I (d); the electrode (a) in the presence of hemin, N. BstNB I and TD (e) in a 100 mM Tris–HCl solution containing 0.1 M KCl and 2 mM H_2O_2.

Another question arises as to whether the formed G-quadruplex-hemin DNAzyme could catalyze the reduction of H_2O_2 in the solution to amplify the electrochemical signal of the adsorbed MB. To investigate this issue, we studied the electrochemical behavior of S2-CP-AuNP/S1/CS–GR/GCE after interacted with 1 nM TD and N.BstNB I nicking. As can be seen in Fig. 3, no redox peaks were observed after the resulting biosensor was incubated with hemin (curve a). When the resulting biosensor was incubated with hemin and MB, a pair of redox peaks was observed (curve b). Favorably, upon addition of 2 mM H_2O_2 in Tris–HCl, an obvious catalytic characteristic appeared with a dramatic increase of peak current (curve c). The result indicated that the formed G-quadruplex-hemin DNAzyme could exhibit an obvious enzymatic catalytic behavior. The increase of the peak current was mainly derived from the G-quadruplex-hemin DNAzyme toward the catalytic reduction of H_2O_2 with the help of MB electron mediators. Hence, the G-quadruplex-hemin DNAzyme could be used for the signal amplification in this biosensing system.

To verify the signal amplification role of CS–GR and AuNP in this as-prepared S2-CP-AuNP/S1/CS–GR/GCE, we prepared another two types of secondary biosensors, i.e., S2-CP-AuNP/S1/GCE (A), CP/CS–GR/GCE (B) under the same experimental conditions. The DPVs of different modified electrodes are displayed in Fig. 4. Curve a in Fig. 4A–C shows the DPVs of different biosensors in the presence of hemin and N.BstNB I but without TD. Curve b in Fig. 4A–C

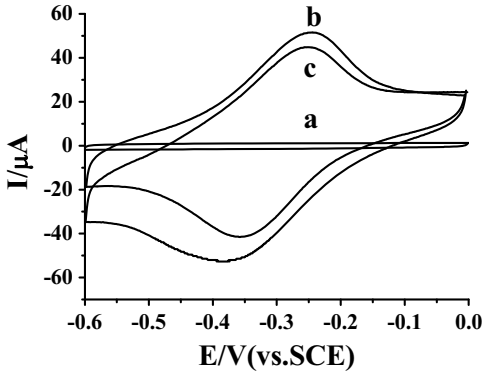

Fig. 3. CVs of as prepared S2-CP-AuNP/S1/CS–GR/GCE after interacted with 1 nM TD and N.BstNB I nicking: incubated with hemin (a); incubated with hemin and MB (b and c) in the absence (b) or in the presence of (a and c) 2 mM H_2O_2 in Tris–HCl (100 mM, pH 7.4, containing 0.1 M KCl).

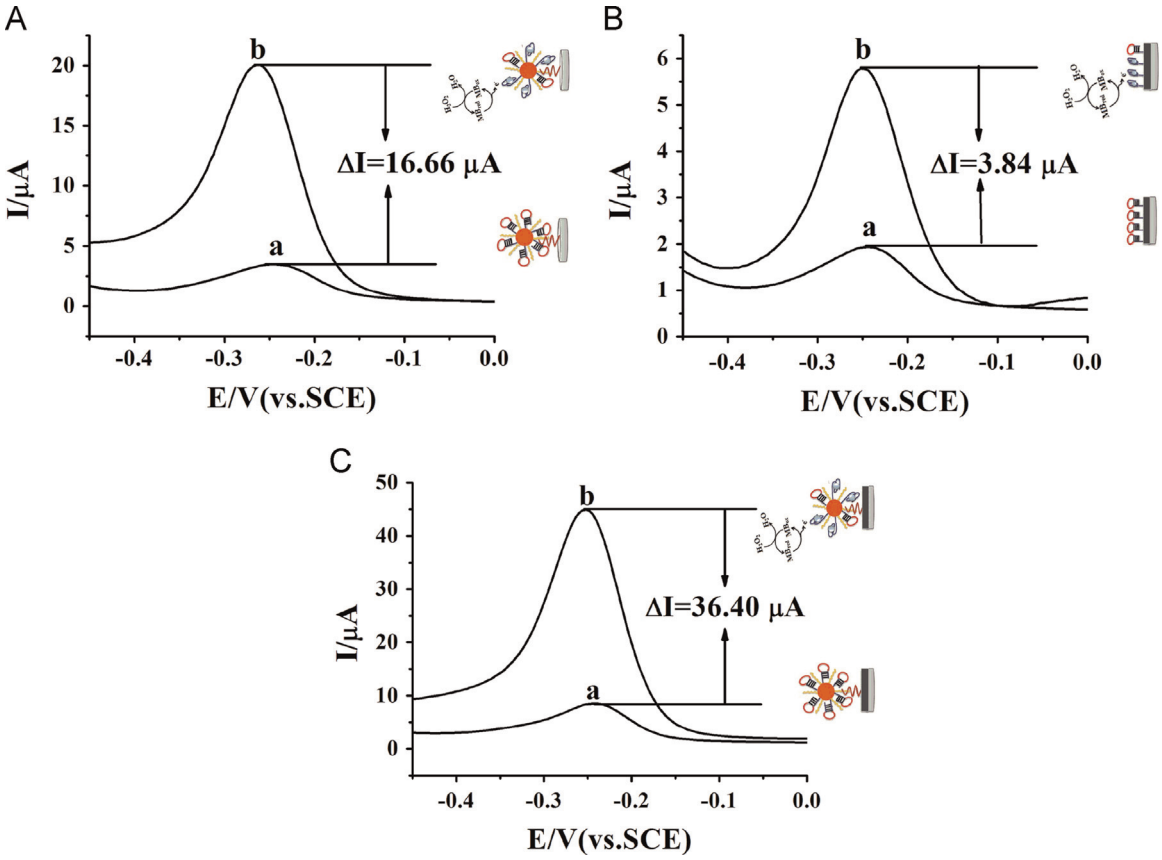

Fig. 4. DPVs of S2-CP-AuNP/S1/GCE (A), CP/CS–GR/GCE (B) and S2-CP-AuNP/S1/CS–GR/GCE (C) towards detecting of TD (in the absence of TD (curve a) and in the presence of TD (curve b)) in Tris–HCl (100 mM, pH 7.4, containing 0.1 M KCl and 2 mM H_2O_2).

shows the DPVs of these three electrodes in the presence of hemin, N.BstNB I and TD. It was obvious that the difference between the peak currents of curve a and curve b in Fig. 4C was the largest, which may attribute to the following reasons: Firstly, the employment of CS–GR with excellent conductivity can provide a large surface for the immobilization of probe DNA and enhance the electrocatalytic efficiency of AuNPs and G-quadruplex-hemin DNAzyme. Secondly, the as-prepared AuNPs with large surface area not only act as a biomaterial to immobilize large amount of CP, G-quadruplex-hemin DNAzyme and MB, but also show remarkable catalytic activity toward H_2O_2 reduction. Furthermore, the synergetic catalysis of AuNPs and G-quadruplex-hemin DNAzyme finally resulted in the greatly amplified detection signal and prominent sensitivity of the proposed biosensor.

On the basis of these above results, we might clearly observe that the quadruple siganl amplification of the electrochemical biosensor could be implemented by using N.BstNB I, G-quadruplex-hemin DNAzyme, CS–GR and AuNPs.

3.5. Optimization of experimental conditions

To achieve superior sensitivity, assay parameters such as the time of TD interaction, the pH of the detection buffer, the concentration of H_2O_2 and hemin were investigated in this work. As shown in Fig. S3(A), the biosensor was incubated with TD (1 nM) for a certain period of time ranging from 20 to 120 min. After that, the biosensor was treated with N.BstNB I and hemin. The DPV response signal increased with increased incubation time and then reached equilibrium after about 80 min. Taking account of efficiency, 80 min was chosen as the optimal incubation time. Fig. S3 (B) shows the effects of pH of the detection buffer on the DPV response. Optimal response for TD detections is obtained at pH 7.4, which is selected for the following experiments. For H_2O_2, DPV response signal is increased with increasing H_2O_2 concentration, and reaches the highest at 2 mM, and then decreases (Fig. S3(C)). For hemin, DPV response signal is also increased with hemin concentration increasing, and reaches equilibrium after about 0.2 mM (Fig. S3 (D)). To guarantee the maximal formation of the G-quadruplex-hemin DNAzyme, the amount of hemin was settled at 0.2 mM.

3.6. Target DNA sensing

Under the optimal conditions, the sensitivity of the assay based on CS–GR, AuNPs, G-quadruplex-hemin DNAzyme and the N. BstNB I-assisted target recycling was investigated by varying the target concentration. As displayed in Fig. 5A, the electrochemical response was very sensitive to the change in the TD concentration and increased with the increase in the concentration of TD, and the peak currents was found to be logarithmically related to the concentration of TD in the range from 1.0×10^{-15}–1.02×10^{-9} M ($I = 81.76 + 4.417 \log C$ $R = 0.9930$, Fig. 5B). The detection limit (LOD) estimated to be 3.0×10^{-16} M (3σ, σ is the relation standard deviation of a blank solution). A comparison has been made between the proposed assay and other reported electrochemical signal amplification methods (Table S1). The above results showed that the integration of CS–GR, AuNPs, N.BstNB I and G-quadruplex-hemin DNAzyme could provide a possible enhancement of electrochemical signals and improvement of sensitivity, as expected. As compared to other methods, this method possessed good sensitivity, though it is lower than several methods. In addition, the innovative advantage of this method is the exploration for quadruple signal amplification strategy. Moreover, the GR used in this method, which have the property of large surface area and

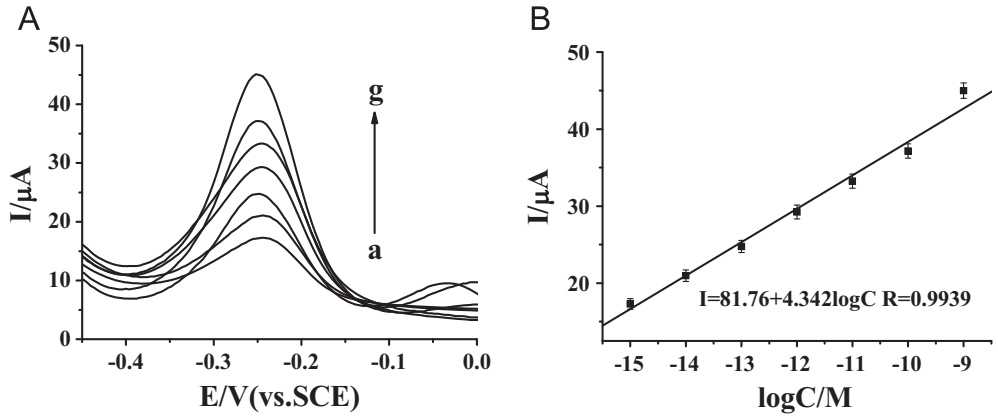

Fig. 5. (A) DPVs for S2-CP-AuNP/S1/CS–GR/GCE detection of different concentrations (a–g: 10^{-15} M, 10^{-14} M, 10^{-13} M, 10^{-12} M, 10^{-11} M, 10^{-10} M, 10^{-9} M) of TD; (B) Linear relationship between the peak currents and the logarithm of TD concentration.

easy-modified, can be further functinalized to improve the analytical performances of the biosensor.

3.7. Specificity, reproducibility and stability

The specificity of the proposed assay was investigated by exposing the sensor to the same concentration of three different kinds of DNA sequences, the perfect complementary sequences (TD), signal-base mismatch sequence (sTD) and non-complementary sequence (nTD), respectively (Fig. S4). As anticipated, the highest peak current increment (ΔI) was observed after hybridization with TD. However, when hybridized with sTD and the nTD, the ΔI changes slightly compared to the blank. These results indicate the advantageous selectivity of our proposed protocol.

The reproducibility of this biosensor was evaluated by the relative standard deviation (RSD, $n=5$) of the signal for 1 nM TD. RSD of 4.14% was obtained using the same electrode to detect TD. RSD of 5.61% was obtained using five different biosensors prepared under the same conditions. These results indicated the good and acceptable reproducibility of the proposed sensor.

The stability of the successive assays was also investigated by carrying out five cycles of DPV measurements with 1 nM TD. The results suggest that peak current decreased by 5.23%. In addition, the long-term storage stability of the proposed protocol was also studied over a three-week period. The DPV peak current retained 95.2% of its initial current after the first week storage and 91.7% after three weeks of storage, respectively, which indicated that the biosensor had a sufficient stability for the detection of TD.

4. Conclusions

In summary, a label-free, ultrasensitive and selective p53 biosensor with quadruple signal amplification strategy resulting from CS–GR, AuNPs, the N.BstNB I-assisted target recycling and G-quadruplex-hemin DNAzyme catalyzing has been developed. The CS–GR with increased surface area and improved electron transfer ability served as an ideal nano-carrier led to the attachment of large amounts of AuNPs-DNA on the electrode surface, paving the way for the amplified electrochemical detection. With the N.BstNB I-assisted target recycling, more G-quadruplex-hemin DNAzymes intercalated with electron mediator MB which exempts the assay from conventional cumbersome labeling could be formed and the co-electrocatalytic behavior of AuNPs with G-quadruplex-hemin DNAzyme greatly amplified the detection signal, achieving high sensitivity of the biosensor. With advantages such as wide linear range, high sensitivity and good selectivity, this strategy has the potential to be integrated in portable for diagnostic applications.

Acknowledgments

We greatly appreciate the financial support from the National Natural Science Foundation of China (21405086, 21475071, 21275082, 81102411 and 21203228), the National Key Basic Research Development Program of China (973 special preliminary study plan, Grant no.: 2012CB722705), the Taishan Scholar Program of Shandong Province and the Natural Science Foundation of Qingdao (13-1-4-128-jch and 13-1-4-202-jch).

Appendix A. Supplementary material

Supplementary data associated with this article can be found in the online version at http://dx.doi.org/10.1016/j.bios.2015.09.011.

References

Breaker, R.R., 2000. Science 290, 2095–2096.
Brownson, D.A.C., Kampouris, D.K., Banks, C.E., 2012. Chem. Soc. Rev. 41, 6944–6976.
Chen, F., Wang, W., El-Deiry, W.S., 2010. Biochem. Pharmacol. 80, 724–730.
Chen, H., Muller, M.B., Gilmore, K.J., Wallace, G.G., Li, D., 2008. Adv. Mater. 20, 3557–3561.
Chen, Y., Wang, Q., Xu, J., Xiang, Y., Yuan, R., Chai, Y.Q., 2013. Chem. Commun. 49, 2052–2054.
Deng, M., Zhang, D., Zhou, Y., Zhou, X., 2008. J. Am. Chem. Soc. 130, 13095–13102.
Deng, S.Y., Cheng, L.X., Lei, J.P., Cheng, Y., Huang, Y., Ju, H.X., 2013. Nanoscale 5, 5435–5441.
Erdem, A., Eksin, E., Muti, M., 2014. Colloids Surf. B 115, 205–211.
Gao, Y., Li, B.X., 2013. Anal. Chem. 85, 11494–11500.
He, Q.Y., Wu, S.X., Yin, Z.Y., Zhang, H., 2012. Chem. Sci. 3, 1764–1772.
Johnson, R.R., Johnson, A.T.C., Klein, M.L., 2008. Nano Lett. 8, 69–75.
Jungemann, A.H., Harimech, P.K., Brown, T., Kanaras, A.G., 2013. Nanoscale. 5, 9503–9510.
Kang, X.H., Wang, J., Wu, H., Aksay, I.A., Liu, J., Lin, Y.H., 2009. Biosens. Bioelectron. 25, 901–905.
Lee, J.H., Jang, H., Cho, E.J., Youn, H.D., 2009. Biochem. Biophys. Res. Commun. 389, 399–404.
Lee, L.G., Connell, C.R., Bloch, W., 1993. Nucl. Acids Res. 21, 3761–3766.
Li, J.S., Deng, T., Chu, X., Yang, R.H., Jiang, J.H., Shen, G.L., Yu, R.Q., 2010. Anal. Chem. 82, 2811–2816.
Liu, B.Q., Zhang, B., Chen, G.N., Tang, D.P., 2014. Chem. Commun. 50, 1900–1902.
Liu, J.W., Lu, Y., 2006. Nat. Protoc. 1, 246–252.
Liu, S.F., Wang, C.F., Zhang, C.X., Wang, Y., Tang, B., 2013a. Anal. Chem. 85, 2282–2288.
Liu, Y.H., Li, H.N., Chen, W., Liu, A.L., Lin, X.H., Chen, Y.Z., 2013b. Anal. Chem. 85, 273–277.
Miao, P., Ning, L.M., Li, X.X., 2013. Anal. Chem. 85, 7966–7970.
Paleček, E., Bartošík, M., 2012. Chem. Rev. 112, 3427–3481.

Pelossof, G., Tel-Vered, R., Elbaz, J., Willner, I., 2010. Anal. Chem. 82, 4396–4402.
Pelossof, G., Tel-Vered, R., Willner, I., 2012. Anal. Chem. 84, 3703–3709.
Qiu, L.P., Qiu, L., Wu, Z.S., Shen, G.L., Yu, R.Q., 2013. Anal. Chem. 85, 8225–8231.
Rosi, N., Mirkin, C., 2005. Chem. Rev. 105, 1547–1562.
Singh, A., Sinsinbar, G., Choudhary, M., Kumar, V., Pasricha, R., Verma, H.N., Singh, S. P., Arora, K., 2013. Sens. Actuators B 185, 675–684.
Wang, G.F., Xu, G., Zhu, Y.H., Zhang, X.J., 2014. Chem. Commun. 50, 747–750.
Wang, Z.H., Xia, J.F., Zhu, L.Y., Zhang, F.F., Guo, X.M., Li, Y.H., Xia, Y.Z., 2012. Sens. Actuators B 161, 131–136.
Wu, Z., Zhen, Z.K., Tang, H., Tang, L.J., Jiang, J.H., 2013. Anal. Chem. 85, 4376–4383.
Xu, G.Y., Jiao, K., Fan, J.S., Sun, W., 2006. Acta Chim. Slov. 53, 486–491.
Xu, M.D., Zhuang, J.Y., Chen, X., Chen, G.N., Tang, D.P., 2013. Chem. Commun. 49, 7304–7306.
Yao, J., Sun, Y., Yang, M., Duan, Y.X., 2012. J. Mater. Chem. 22, 14313–14329.
Yuan, L., Tu, W.W., Bao, J.C., Dai, Z.H., 2015. Anal. Chem., 686–692.
Yuan, Y.L., Chai, Y.Q., Yuan, R., Zhuo, Y., Gan, X.X., 2013. Chem. Commun. 49, 7328–7330.
Zhang, F.T., Nie, J., Zhang, D.W., Chen, J.T., Zhou, Y.L., Zhang, X.X., 2014a. Anal. Chem., 9489–9495.
Zhang, J., Chai, Y.Q., Yuan, R., Yuan, Y.L., Bai, L.J., Xie, S.B., Jiang, L.P., 2013. Analyst 138, 4558–4564.
Zhang, K., Wang, K., Zhu, X., Zhang, J., Xu, L., Huang, B., Xie, M.H., 2014b. Chem. Commun. 50, 180–182.
Zheng, Y.N., Chai, Y.Q., Yuan, Y.L., Yuan, R., 2014. Anal. Chim. Acta, 45–50.
Zhou, H., Zhang, Y.Y., Liu, J., Xu, J.J., Chen, H.Y., 2013. Chem.Commun. 49, 2246–2248.
Zhou, M.Y., Liu, Y., Tu, Y.F., Tao, G.H., Yan, J.L., 2012. Biosens. Bioelectron. 35, 489–492.
Zhu, G.C., Li, Y., Zhang, C.Y., 2014. Chem. Commun. 50, 572–574.